

Article

Global Characterization of XRN 5'-3' Exoribonucleases and Their Responses to Environmental Stresses in Plants

Weimeng Song^{1,2}, Yanjie Li³, Yue Niu³, You Wu⁴, Yan Bao^{3,*} and Xiang Yu^{4,*} 

¹ State Key Laboratory for Conservation and Utilization of Subtropical Agro-Bioresources, South China Agriculture University, Guangzhou 510642, China; wmsong@scau.edu.cn

² Guangdong Key Laboratory for Innovative Development and Utilization of Forest Plant Germplasm, College of Forestry and Landscape Architecture, South China Agricultural University, Guangzhou 510642, China

³ Joint Center for Single Cell Biology, School of Agriculture and Biology, Shanghai Jiao Tong University, Shanghai 200240, China; angie8008@sjtu.edu.cn (Y.L.); ny905319991@163.com (Y.N.)

⁴ School of Life Sciences and Biotechnology, Shanghai Jiao Tong University, Shanghai 200240, China; Wuyou1990@sjtu.edu.cn

* Correspondence: yanbao@sjtu.edu.cn (Y.B.); yuxiang2021@sjtu.edu.cn (X.Y.)

Abstract: The XRN family of 5'-3' Exoribonucleases is functionally conserved in eukaryotic organisms. However, the molecular evolution of XRN proteins in plants and their functions in plant response to environment stresses remain largely unexplored. In this study, we identified 23 XRN proteins in 6 representative plant species. Polygenetic analysis revealed that XRN2 was Arabidopsis-specific among these species, and additional branches outside the clades of XRN3 and XRN4 proteins, which we named as XRN5, were found in rice, maize, and soybean. However, XRN5 in soybean lost their entire 5'-3' XRN Exoribonuclease domain. Protein conserved sequence analysis showed that XRN3/XRN2 contained potential bipartite nuclear-localization signals (NLS) while all the XRN4 proteins lost their second KR/RR motif of NLS, potentially leading to their cytoplasm localization. SIXRN3-2 contained one mutation in this second KR/RR motif, which may change their sub-cellular localization. The promoter cis-element analysis indicated that these XRN genes responded to multiple stresses and plant hormones diversely at transcriptional level. Finally, transcriptomic analysis suggested that *OsXRN3* and *ZmXRN3-1* were induced by low temperature, *SIXRN4* and *ZmXRN4* was inhibited by heat shock, and *OsXRN5* and *GmXRN5-2* were repressed by drought. However, in general, the expression patterns revealed the response diversity of XRNs to environment stimuli in different plant species. Taken together, this study characterized 23 XRNs with NLS variation that contributed to their sub-cellular localization and provided an overview of the XRNs response diversity to multiple environmental stresses, suggesting that XRNs could be used as potential gene editing candidates for precise stress-tolerant crop breeding.

Keywords: 5'-3' exonuclease; XRNs; nuclear-localization signals; stress response diversity; polygenetic analysis



Citation: Song, W.; Li, Y.; Niu, Y.; Wu, Y.; Bao, Y.; Yu, X. Global Characterization of XRN 5'-3' Exoribonucleases and Their Responses to Environmental Stresses in Plants. *Diversity* **2021**, *13*, 612. <https://doi.org/10.3390/d13120612>

Academic Editor: Mario A. Pagnotta

Received: 26 October 2021

Accepted: 23 November 2021

Published: 24 November 2021

Publisher's Note: MDPI stays neutral with regard to jurisdictional claims in published maps and institutional affiliations.



Copyright: © 2021 by the authors. Licensee MDPI, Basel, Switzerland. This article is an open access article distributed under the terms and conditions of the Creative Commons Attribution (CC BY) license (<https://creativecommons.org/licenses/by/4.0/>).

1. Introduction

RNA degradation plays a critical role in RNA quantity and quality control. In general, RNA turnover is triggered by 3' polyA tail shortening and 5' cap removal, followed by Exoribonucleases cleavage from 5' to 3' and/or from 3' to 5' [1]. In yeast, there are two XRN of 5'-3' exoribonucleases: cytoplasmic enzyme XRN1 and nuclear enzyme XRN2 [2]. XRN1 plays a role in cytoplasmic RNA decay, whose substrates include mRNAs, noncoding RNAs and products from Nonsense-mediated mRNA decay, while XRN2 (Rat1) functions in nuclear RNA decay with its activating partner RAI1 [3,4]. Current studies also suggested that yeast XRN1 can degrade the mRNA following the last ribosome in a co-translational RNA decay manner [5].

In Arabidopsis, 5'-3' Exoribonucleases include three XRN: AtXRN2, AtXRN3 and AtXRN4, which are homologs of yeast XRN2, lacking yeast homologous gene XRN1 [6].

Nuclear localization signals (NLS) are important for the protein import into the nucleus. NLS generally contain a high content of basic amino acids arginine (R) and Lysine (K), but without strict consensus sequence [7]. AtXRN2 and AtXRN3 contain the bipartite NLS and play a role in degrading ribosome RNAs or other aberrant RNAs in the nucleus; interestingly, AtXRN4 loses the second part of bipartite NLS, leading to its change in sub-cellular localization, and degrades mRNAs in cytoplasm [6,8]. Current studies also revealed that AtXRN4 was involved in co-translational RNA decay [9–11], and AtXRN3 mediated transcription termination of protein-coding genes in Arabidopsis [12].

In plants, XRNs play critical roles in non-coding RNA pathways [13]. Disruption of XRNs and other RNA processing factors results in small RNA-mediated post-transcriptional gene silencing (PTGS). Therefore, XRNs are considered as the repressors of PTGS. For instance, mutations in both *XRN4* and *SKI2* cause aberrant RNA accumulation, which trigger PTGS [14]. XRNs also involve in miRNA-mediated RNA turnover. AtXRN4 cleans the 3' products of miRNA-mediated cleavage and affects the turnover of chosen miRNA* in the processing-body [15–18]. Additionally, XRNs function in miRNA processing. AtXRN3, together with FRY1, prevents the accumulation of 3' extensions of DCL1-processed miRNA precursors, and AtXRN2 and AtXRN3 are required for trimming the pri-miRNA stem-loop remnant [19,20].

DXO1, as the homolog of yeast RAI1, has been identified as an NAD⁺ decapping enzyme in Arabidopsis [21,22]. However, whether DXO1 could interact with XRNs in Arabidopsis have not been investigated. Furthermore, current study suggested XRNs in animals could function in the removal of RNA NAD⁺ cap modification [23]. Whether this function is conserved in the plant remains unclear.

The three *AtXRN*s are expressed in most of the organs in Arabidopsis [6]. AtXRN4 contributes to ethylene signal transduction and the regulation of ABA signaling [24,25], and it is required for heat-triggered co-translational RNA decay in plant response to heat stress [9,26]. Recent studies also suggest that AtXRN4 is important for plant response to dark and nitrogen stress [27]. However, the functions of AtXRN2 and AtXRN3 in plant response to abiotic and biotic stress are still unknown. The characterization of XRNs in other plants and the response of XRNs to environmental stress in other plant species remain largely unexplored. In this study, we aimed to identify global XRNs in representative species for investigating their molecular evolution and potential functions in plant response to stresses.

2. Materials and Methods

2.1. Genome-Wide Identification and Characterization of XRN Proteins

The genome and gene annotation files of Arabidopsis (version Araport11), soybean (version Wm82.a4), tomato (version ITAG3.2), rice (version MSUv7.0), maize (version 6a), and moss (version 3.3) were downloaded from phytozome (<https://phytozome-next.jgi.doe.gov/>, accessed on 11 October 2021). Proteins that are putative homologs of AtXRN2, AtXRN3, and AtXRN4 were identified based on hmm search from Phytozome v13.

2.2. Construction of Polygenetic Tree and Gene Structure Visualization

The 23 XRN proteins were aligned by ClusterW method with default parameters embedded in the Molecular Evolutionary Genetics Analysis (MEGA) tool [28]. The polygenetic tree was constructed using neighbor-joining tree with 1000 times of Bootstrap replications in MEGA tool (MEGA X version 10). Genes were labeled with the species names, and their corresponding ID are listed in the result bellowed. The gene annotation of XRNs in gff3 files were extracted and the gene structure visualization were performed using Toolbox for biologists (TBtools) [29].

2.3. Calculation of Biochemical Properties of XRN Proteins

The molecular weight (MW) and theoretical isoelectric point (pI) of XRN proteins was calculated using the Compute pI/Mw tool (https://web.expasy.org/compute_pi/, accessed on 11 October 2021) using the XRN protein sequences as input.

2.4. Conserved Protein Motif and Domain Analysis

The protein sequences of 23 XRN proteins from 6 species were uploaded to MEME website (<https://meme-suite.org/meme/tools/meme>, accessed on 11 October 2021) for motif discovery, searching for 30 conserved protein motifs. The XML file of motif discovery result was uploaded to bio-sequences structure illustrators in TBtools for visualizing the motif distribution along the protein sequences. The AtXRN3 protein sequence was used to search conserved domain in NCBI (<https://www.ncbi.nlm.nih.gov/Structure/cdd/wrpsb.cgi>, accessed on 11 October 2021), and the XRN 5'-3' exonuclease N-terminus (Pfam03159) was found as the domain possessing 5'-3' exonuclease activity (<https://www.ncbi.nlm.nih.gov/Structure/cdd/cddsrv.cgi?uid=pfam03159>, accessed on 11 October 2021). The protein sequence of bipartite nuclear-localization signal was referred to those in AtXRN proteins [6], which was KR-X₁₁-[K|R]RXX.

2.5. Promoter Cis-Element Analysis

The 2-kb promoter sequences of XRN proteins upstream the transcriptional start sites were extracted from the corresponding genome and uploaded to PlantCARE website (<http://bioinformatics.psb.ugent.be/webtools/plantcare/html/>, accessed on 11 October 2021) for searching cis-acting regulatory elements in these promoter sequences [30]. The motif distribution along the 2-kb promoters were visualized by TBtools.

2.6. Transcriptome Analysis for XRN Proteins

The transcriptome data of Moss, Tomato, Soybean, Rice, and Maize was collected from the database of *Physcomitrella patens* gene atlas project, Tomexpress (<http://tomexpress.toulouse.inra.fr/>, accessed on 11 October 2021), Soybean Expression Atlas (http://venanciogroup.uenf.br/cgi-bin/gmax_atlas/download_by_tissue.cgi, accessed on 11 October 2021), Transcriptome Encyclopedia of Rice (tenor.dna.affrc.go.jp, 11 October 2021), and Maize Genomics Resource (<http://maize.uga.edu/index.shtml>, accessed on 11 October 2021), respectively [31–35]. The relative fold change of XRN RNA abundance under different stresses or treatments related to the control was visualized by heatmap using R package pheatmap.

2.7. XRN Protein Structure Prediction and Pairwise Structure Alignment

The protein sequences of XRN proteins were uploaded to SJTU High Performance Computing (HPC) center for 3D structure prediction using AlphaFold2 [36]. The pairwise structure alignment was performed using the online tool in Protein Data Bank (<https://www.rcsb.org/alignment>, accessed on 15 November 2021).

3. Results

3.1. Identification and Characterization of XRN Proteins in Plant Species

To characterize XRN proteins in plant species, the protein sequences of AtXRN2, AtXRN3 and AtXRN4 were used to identify potential homologs based on hmmsearch in Phytozome. In total, we identified 23 putative homologs of XRN proteins in 6 representative plant species, including three dicots: *Arabidopsis*, tomato, soybean; two monocots: rice and maize, and one moss: *Physcomitrella patens* (Table 1). The protein length of XRN proteins ranged from 413 to 1118 aa (amino acids). We further calculated their molecular weight (MW) and isoelectric point (pI). The pI of XRN proteins varied from 5.78 to 8.99, and MW of XRN proteins were between 46.62 Da and 126.98 Da. These results indicated the diversity of biochemical properties in protein length, MW and pI among plant XRN homologs.

Table 1. The summary of 23 XRN proteins in 6 plant species, including their gene ID, gene name, exon number, gene length, CDS length, protein length, pI, and MW.

	Gene ID	Gene Name	Exon Number	Gene Length (bp)	CDS Length (bp)	Protein Length (aa)	pI	MW(kDa)
1	LOC_Os01g65220	OsXRN3	23	7877	3207	1068	6.81	120.83
2	GRMZM2G064868	ZmXRN3-1	9	13,437	3240	1079	6.94	122.50
3	GRMZM2G121404	ZmXRN3-2	14	6709	3201	1066	6.83	120.70
4	Glyma.14G218000	GmXRN3-1	23	11,147	3246	1081	6.85	123.09
5	Glyma.17G257100	GmXRN3-2	23	11,870	3210	1069	7.02	121.71
6	Solyc04g081280.3	SIXRN3-1	23	13,091	3330	1109	5.97	126.46
7	Solyc12g089280.2	SIXRN3-2	23	20,707	3351	1116	8.85	126.98
8	AT1G75660	AtXRN3	23	6985	3063	1020	6.53	116.83
9	AT5G42540	AtXRN2	22	7481	3072	1023	8.99	117.69
10	Pp3c14_10280	PpXRN3-1	23	10,353	3000	999	6.38	112.98
11	Pp3c24_2160	PpXRN3-2	14	7360	3357	1118	6.24	126.21
12	GRMZM2G099630	ZmXRN4	22	15,261	2973	990	7.39	113.31
13	LOC_Os03g58060	OsXRN4	22	11,089	2967	988	7.88	112.64
14	AT1G54490	AtXRN4	22	6808	2844	947	6.37	107.78
15	Solyc04g049010.3	SIXRN4	23	41,681	2937	978	7.09	111.57
16	Glyma.20G228700	GmXRN4-1	22	10,058	2799	932	6.46	107.14
17	Glyma.03G245000	GmXRN4-2	22	12,844	2886	961	6.37	109.90
18	Glyma.19G242400	GmXRN4-3	22	12,523	2877	958	6.48	109.94
19	GRMZM2G458401	ZmXRN5-1	23	6136	2682	893	7.77	101.60
20	GRMZM2G046755	ZmXRN5-2	21	5370	2388	795	5.78	90.67
21	LOC_Os02g28074	OsXRN5	21	16,540	2469	822	6.17	93.70
22	Glyma.11G180000	GmXRN5-1	15	5039	1659	552	8.68	63.20
23	Glyma.12G093500	GmXRN5-2	9	2848	1242	413	8.45	46.62

Next, the phylogenetic analysis of these XRN proteins was performed based on the XRN protein sequences. In the clade of XRN2 and XRN3 proteins, the phylogenetic tree showed that moss, tomato, soybean, and maize contained two XRN3 copies, while XRN2 protein only existed in Arabidopsis (Figure 1). We further analyzed the structure similarity of XRN3 proteins predicted by AlphaFold2 between monocot and dicot using OsXRN3 and AtXRN3 as representative. The pairwise structure alignment showed that 777 residue pairs were structurally equivalent between these two XRN3 proteins (Figure S1). For the clade of XRN4 proteins, we found three XRN4 proteins in soybean, one XRN4 in Arabidopsis, tomato, rice, and maize, but no XRN4 proteins were found in moss. Interestingly, additional branches of XRN proteins outside the clades of XRN3 and XRN4 were found in rice, maize, and soybean, which we named as XRN5. There were two XRN5 homologous genes in maize and soybean. Taken together, we found that XRN3 proteins were conserved from moss to angiosperm plants and triplicated in soybean, XRN2 protein only existed in Arabidopsis among these 6 species, and XRN4 proteins were conserved in flowering plants, but not in moss; additionally, XRN5 proteins were uncovered in monocot rice and maize and dicot soybean.

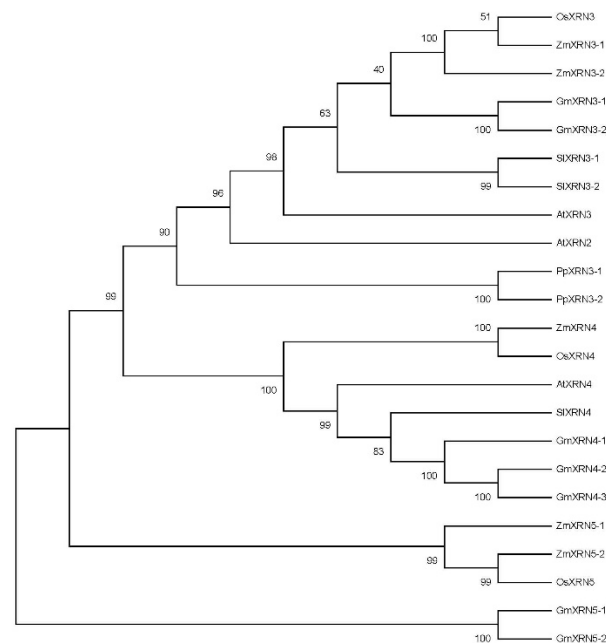


Figure 1. The polygenetic analysis of XRN3s in moss, Arabidopsis, tomato, soybean, rice, and maize. The sequences were aligned by ClusterW method, and the polygenetic tree was constructed using the NJ method in MEGA tool with 1000 bootstrap replicates. The numbers above the branches refer to the bootstrap value of the neighbor-joining phylogenetic tree.

3.2. Gene Structure Variations in XRN Proteins

To investigate the structural diversity of XRN3s genes in these plant species, we analyzed the exon-intron organization of XRN3s genes by comparing their coding sequences and the corresponding genomic sequences. Firstly, we explored the exon number in these XRN3s genes. The number of exons in the XRN3s genes varied from 9 to 23, and 18 of 23 XRN3s had more than 20 exons (Table 1 and Figure 2). For the gene structure of XRN3, 7 out of the 10 XRN3 genes contained 23 exons, while ZmXRN3-2 and PpXRN3-2 genes had 14 exons and ZmXRN3-1 had 9 exons. For the XRN4 genes, all had 22 exons except SIXRN4, which contained 23 exons. For the XRN5 genes, their exon numbers showed high diversity. The monocot XRN5 including OsXRN5 and ZmXRN5-2, which had 21 exons, while ZmXRN5-1 contained 23 exons. In dicot soybean, there were 15 exons in GmXRN5-1 and 9 exons in GmXRN5-2. Further, the XRN3s genes that clustered together exhibit similar exon-intron organization, which was consistent with the results of our phylogenetic analysis (Figure 2).

Next, we analyzed the gene length of these XRN3s. The gene length of GmXRN5-2 was around 2848 bp, which is the shortest, while SIXRN4 gene length was the longest with around 41,681 bp. Interestingly, SIXRN3-2 was also the longest gene in all these XRN3 genes, while OsXRN5 was the longest gene in all these XRN5 genes. Given that most of the XRN3s contain more than 20 exons and their CDS length is not particularly diverse, we found that the expansion of intron length contributed most significantly to the gene length of these long XRN3s genes, while loss of exons causing truncated proteins contributed to the shortness of those XRN3s with small gene size. Taken together, we found these XRN3s were diverse in exon number and gene length.

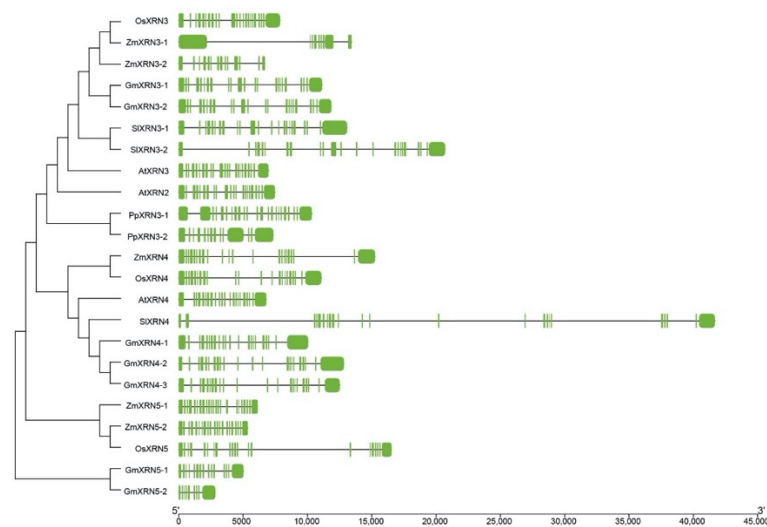


Figure 2. The gene structure of XRN proteins in 6 plant species displaying with the same order as phylogenetic tree. Exons and introns are shown as green boxes and black lines, respectively.

3.3. Characterization of Conserved Motifs and NLS in XRN

To further study the conserved and novel functional domains of these XRN proteins, we searched conserved amino acid sequences via MEME tool and identified 30 enriched motifs. Interestingly, we found all these XRN proteins contained motif 15 (Figure 3A and Figure S2A). Most of the XRN3 proteins contained 27 conserved motifs, while XRN2 lost motifs 10, 30, and 22 (Figure 3A). Some XRN3 also lost a few motifs. For instance, we found that SIXRN3-2 lost the motif 26 and PpXRN3-1 lost motifs 22 and 26. As compared to XRN3, we found that all the XRN4 proteins lost motifs 30, 22, 26 and 19, which were clustered together (Figure 3A and Figure S2B), but contained unique motifs 27 and 29 (Figure S2C). Instead, XRN5 protein lost motifs 14, 16, 30, 22, 26, 25, 8, 23 and 20, but specifically contained motif 24 (Figure 3A and Figure S2D). Taken together, we characterized the conserved motifs that were distributed in these XRN proteins.

Next, we wanted to clarify which protein functional domain has XRN 5'-3' exonuclease activity. To do this, we aligned the AtXRN3 protein sequence to the database of conserved domains in NCBI. The result showed that the N-terminus of AtXRN3 conserved with the pfam03159 domain, which possesses 5'-3' exonuclease activity (Figure S3A). We further checked the similarity between this conserved domain and identified motifs and found that this N-terminus domain included the motifs 14, 7, 4, 9, 21, 6, 18, and 1 (Figure S3A,B). All the XRN3 and XRN4 proteins contained this entire N-terminus domain. However, we found that motif 14 was lost in monocot XRN5, and motif 21 was skipped to another region (Figure 3A). Interestingly, two GmXRN5 proteins in soybean lost all the motifs in XRN 5'-3' exonuclease domain, indicating these two proteins had lost the XRN 5'-3' exonuclease activity.

Previous study suggested that AtXRN2 and AtXRN3 contained the bipartite nuclear-localization signals (NLS), while AtXRN4 lost the second KR/RR motif in NLS [6]. We found that the motif 11 included the first KR motif of bipartite NLS sequences (Figure 3B). This first KR motif was conserved in all the 22 XRN proteins containing motif 11, while all the XRN4 proteins lost the second KR/RR motif, indicating that XRN4 proteins potentially located in cytoplasm and played a role in degrading cytoplasmic RNAs, which was consistent with the function of AtXRN4 in Arabidopsis. Interestingly, we found the second KR/RR motif in SIXRN3-2 contained a mutation and ZmXRN5-2 and GmXRN5-2 lost this KR/RR motif, which may disrupt their nuclear localization (Figure 3C). Additionally, we found XRN3 proteins in higher plants contained a third KR/RR amino acid in motif 30, their effect on protein importing into nucleus remains to be investigated in the future. In

environmental stresses (defense, light, drought, and low temperature) and external plant hormones abscisic acid (ABA), gibberellin (GA), auxin and MeJA were detected among the promoters of these 23 XRNs (Figure 4). Among the stress-responsive cis-elements, we found most of the XRN promoters contained light-responsive cis-elements. *OsXRN3* promoters even possessed 6 light-responsive cis-elements. Among the hormone-responsive cis-elements, most of the XRN promoters contained MeJA-responsive cis-elements. For instance, *ZmXRN4* included 5 cis-elements responsive to MeJA. Interestingly, we found some of the XRN3 promoters contained 1 or 2 ABA-responsive cis-elements close to their transcription start site; particularly, both *OsXRN3* and *ZmXRN3-1* contained tandem ABA-responsive cis-elements, indicating a relatively conserved cis-element site in XRN3 promoters. Overall, these data suggest that the diverse transcriptional regulation of XRN genes in responding to multiple biotic and abiotic stimuli.

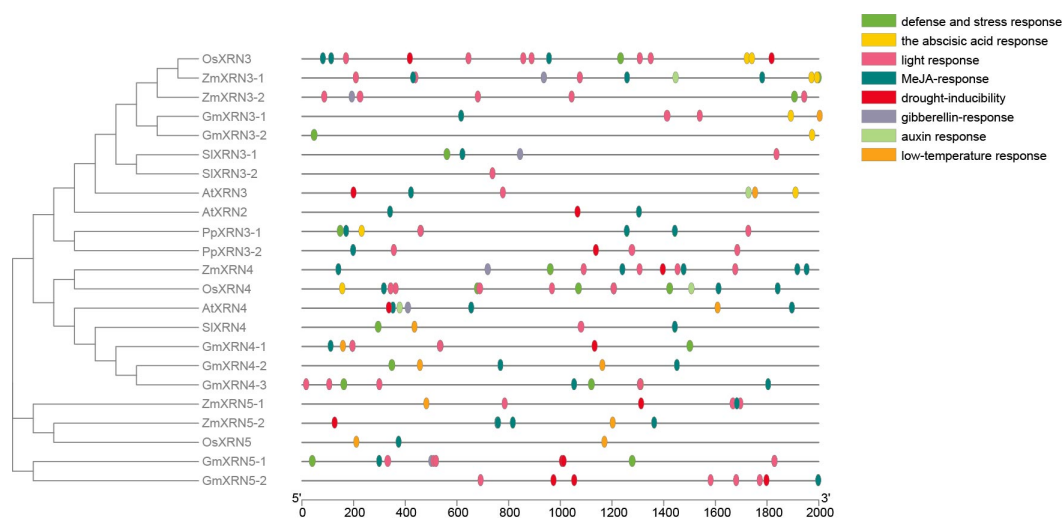


Figure 4. The promoter cis-element analysis of XRN genes in 6 plant species. Differently colored boxes represent the cis elements response to different environmental stresses and plant hormones.

3.5. The Diverse Response of XRNs under Various Environment Stress

Previous studies suggested that XRN4 in *Arabidopsis* functions in diverse stress responses. However, the response of XRNs to various environment stresses in five other species remained largely unexplored. Therefore, we analyzed the expression patterns of XRNs in response to multiple stresses using published transcriptome data. Firstly, we examined the relative RNA abundance of *OsXRNs* in rice shoot and root tissue with cold, flood, osmotic, salt, and drought stress treatments and phytohormones ABA and JA treatments at several different time points. We found both *OsXRN3* and *OsXRN4* was induced by drought stress, while *OsXRN5* was repressed by drought stress in rice shoot (Figure 5A,B). *OsXRN3* was induced by cold stress, showing that the RNA abundance of *OsXRN3* was accumulated highest with 12 h cold treatment in shoot tissue, while it was most abundant after 1d cold treatment in root tissue (Figure 5A,B). Additionally, we found the expression of *OsXRN5* in root tissue was triggered under flood stress. We also examined the response of *OsXRNs* under external plant hormone exposure. The most interesting expression pattern was that *OsXRN5* was gradually repressed by ABA after 1 h, 3 h, 6 h, 12 h, and 24 h (1 d) treatment in rice shoots (Figure 5C). A consistent, very similar down-regulated pattern of *OsXRN5* was observed in rice roots after ABA treatment (Figure 5D). Instead, *OsXRN3* and *OsXRN4* were induced by ABA and JA in rice root tissue (Figure 5D). We further examined the response of *OsXRNs* to cadmium and phosphate and found that cadmium toxicity stress significantly induced *OsXRN4* and *OsXRN5* at transcript level in both shoot and root of rice (Figure S4). Taken together, these results revealed a diverse response of *OsXRNs* under environmental stress and hormone stimuli.

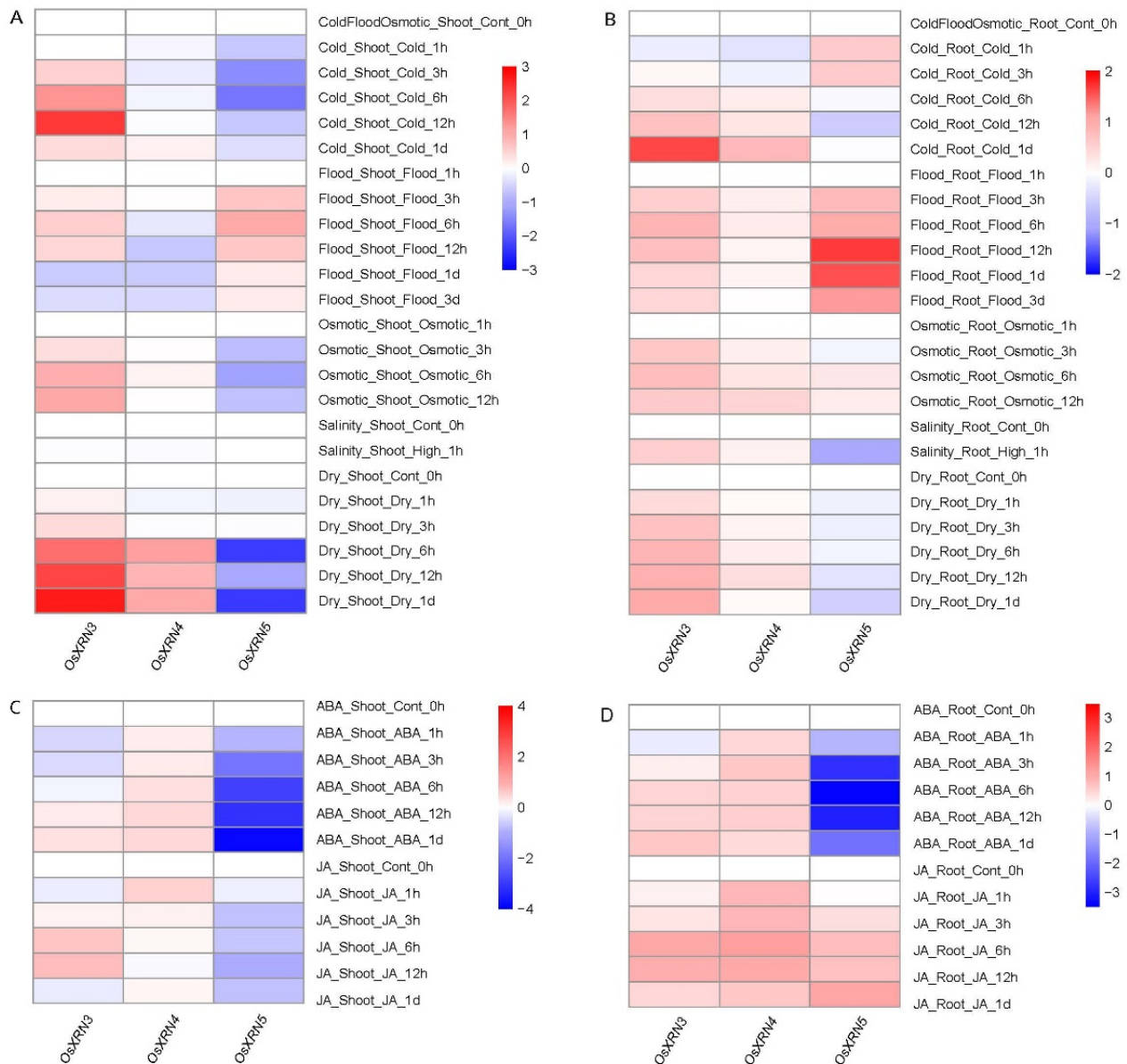


Figure 5. Cluster analysis of the *OsXRN*s expression pattern. (A,B) Heatmap showing expression profiles of *OsXRN*s in response to diverse abiotic stress in rice shoot (A) and root (B). (C,D) Heatmap showing expression profiles of *OsXRN*s in response to phytohormones in rice shoot (C) and root (D). The expression level is represented using color scale ranging from blue (down-regulated) to red (up-regulated).

Next, we examined the expression of XRN genes in another monocot maize, subjecting it to several abiotic stresses. All these transcriptome datasets could not detect *ZmXRN5-1*, indicating it may be a pseudogene. We found all the other *ZmXRN*s were inhibited by heat stress, while *ZmXRN3-1* was induced by low temperature, and *ZmXRN5-2* was repressed by cold stress (Figure 6A). For the dicot soybean, we investigated the response of *GmXRN*s to fungus infection and drought stress. Again, *GmXRN4-1* and *GmXRN5-1* could not be found in the maize transcriptome dataset, indicating these may be pseudogenes. We found that all the *GmXRN*s were repressed by fungus after 96 h (4d) treatment, and the RNA abundance of *GmXRN3-1*, *GmXRN4-3*, and *GmXRN5-2* decreased gradually under drought treatment after 6 h, 12 h, and 24 h (Figure 6B). For another dicot tomato, we found that cytokinin repressed the expression of *SIXRN3-2* and *SIXRN4*, and auxin and ABA induced all these three *SIXRN*s. Interestingly, we found *SIXRN3-1* was inhibited by heat

shock and SIXRN4 was induced by heat shock in both leaf and flower, while SIXRN3-2 increased in leaf but decreased in flower after heat shock (Figure 6C). Finally, we checked the response of moss PpXRNs to drought, heat, and ABA. We found drought induced both PpXRN3-1 and PpXRN3-2, while heat stress specifically repressed PpXRN3-2, and ABA specifically induced PpXRN3-1 (Figure 6D). Taken together, these results revealed the diverse response of these XRNs to multiple environmental stresses and hormone stimuli.

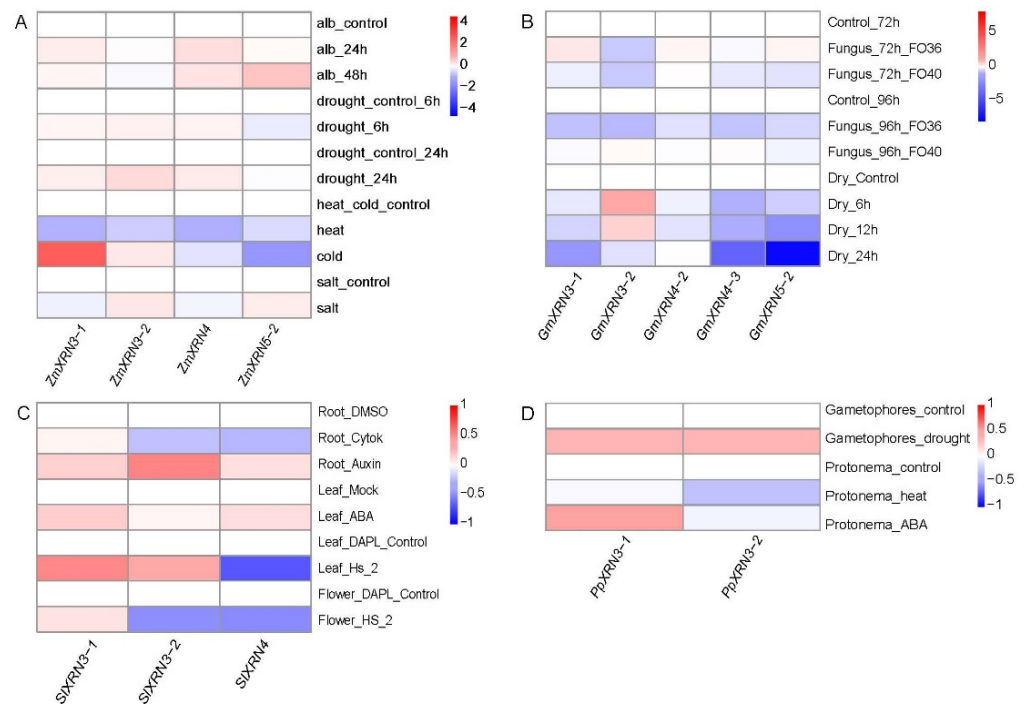


Figure 6. Cluster analysis of the *ZmXRNs*, *GmXRNs*, and *SIXRNs* expression patterns. (A) Heatmap displaying expression profiles of *ZmXRNs* in response to diverse abiotic stress. (B) Heatmap showing expression profiles of *GmXRNs* in response to fungus and Drought treatment. (C) Heatmap showing expression profiles of *SIXRNs* in response to phytohormones and heat shock in different tissues. (D) Heatmap showing expression profiles of *PpXRNs* in response to drought, heat, and ABA.

Finally, we tried to capture the common expression pattern of XRN homologs response to the same environmental stresses in different species. We found that *OsXRN3* and *ZmXRN3-1* were both induced by low temperature, *SIXRN4* and *ZmXRN4* was both inhibited by heat shock, and both *OsXRN5* and *GmXRN5-2* were repressed by drought stress (Figures 5 and 6). In summary, the transcriptomic analysis revealed the stress response conservation and diversity of XRN homologs in different plant species.

4. Discussion

In this study, we characterized 23 XRN proteins from 6 plant species and performed the polygenetic analysis based on their protein sequences to address the molecular evolution of these XRNs. As were known, *Arabidopsis* contained three XRNs: *AtXRN2* and *AtXRN3* that were localized in the nucleus, and *AtXRN4* in the cytoplasm. Interestingly, the homologous genes of *AtXRN2* could not be found in other 5 species studied (Figure 1), but further study is needed to address if its homologous gene could be found in the close relative of *Arabidopsis thaliana*, such as *Arabidopsis lyrata* and *Brassica rapa*. Additional branches of XRNs outside the clades of XRN2/3 and XRN4 proteins were found in monocot rice and maize, which we named as XRN5 (Figure 1). Whether XRN5 proteins are widely spread in monocots need to be further investigated. Interestingly, we found soybean contained two XRN proteins, which were outside all the other clades in the polygenetic

tree, and shared the same motif 24 with monocot XRN5, therefore we also named these two soybean XRN5s as GmXRN5-1 and GmXRN5-2.

We studied the conserved protein motifs in these XRN5s and found motif 15 was conserved in all the XRN5s. XRN3/XRN2 proteins specifically included motifs 30, 22, and 26. XRN4 proteins contained specific motifs 27 and 29, although AtXRN4 in Arabidopsis lost these. XRN5 contained a specific motif 24. Subsequently, we surveyed and found that the conserved N-terminus domain of XRN5s possessing 5'-3' exonuclease activity included several identified motifs cluster together from motif 14 to motif 1. XRN3 and XRN4 proteins contained the whole N-terminus domain, while XRN5 in monocot rice and maize lost motif 14. The GmXRN5 proteins in soybean without the entire N-terminus domain possibly lost their function as 5'-3' exonuclease, and one of them may be the pseudogene.

Next, we focused on the exploration of their potential sub-cellular localization based on the NLS. We found all the XRN4 proteins lost motifs 30, 22, 26, and 19, as compared to that of XRN3 proteins. However, further searching of the bipartite NLS sequences in these motifs showed that, all these 4 motifs did not include the bipartite NLS. Instead, we found the motif 11 upstream of the motif 30 and its flanking region contained the bipartite NLS. Therefore, we investigated the NLS sequences in the multiple alignment results of all these 23 XRN5s. Consistent with the AtXRN4, all the XRN4 contained a large deletion which led to the loss of the second KR/RR motif of NLS. Interestingly, all the XRN5 with motif 11 contained a small deletion, causing the disruption of the second [K|R][K|R]XR motif. In the clade of XRN3, SIXRN3-2 contained one mutation in the second KR/RR motif of NLS. Overall, more detailed experiments need to be performed to address the effect of the mutation in bipartite NLS on the sub-cellular localization of these XRN5s. We also noticed that the moss *Physcomitrella patens* contained two XRN3 proteins but not XRN4. This observation opens a window for several interesting questions: whether these two XRN3 proteins containing NLS could partially localize in the cytoplasm for cytoplasmic mRNA degradation? When was a cytoplasm-localized XRN4 protein evolved? Characterization of XRN5s in more plant genomes such as ferns could address the last question.

Finally, we studied the response of these XRN5s to multiple abiotic and biotic stresses. We found drought stress both repressed the transcription of *OsXRN5* in rice and *GmXRN5-2* in soybean. However, drought inhibited the expression of *GmXRN3-1* and *GmXRN4-3* in soybean, but induced *OsXRN3* and *OsXRN4* in rice, indicating a diverse response of XRN5 homologs to the same stress stimuli, which was consistent with the distribution diversity of drought-responsive cis-elements in their promoters of these XRN5s. In Arabidopsis, XRN4 contributed to heat-induced co-translational RNA decay under heat stress. However, we found both *SIXRN4* and *ZmXRN4* were repressed by high temperature. In addition, we found low temperature induced the expression of both *OsXRN3* and *ZmXRN3*. Taken together, the transcriptomic analysis suggested the diverse response of XRN5 homologs to environmental stresses in different species.

Overall, we provided a global view of the XRN5 proteins in 6 representative plant species. Currently, little genetic studies related to the eco-physiology and biochemical response of XRN5s were carried out in non-model plant species. In the future, mutation in XRN5s could be induced by gene editing using CRISPR technology in other species such as rice and tomato. In Arabidopsis, XRN4 functions in ethylene and ABA signaling pathways, and is involved in heat-response [9,24–26]. The crosstalk between hormone signaling pathways and stress-response pathways mediated by XRN4 remains to be further investigated. XRN4 play role in cytoplasmic RNA decay, co-translational RNA decay and potentially NAD⁺ decapping [9–11,23]. In contrast, XRN2 and XRN3 proteins function in nuclear RNA processing and degradation, including pre-ribosomal RNAs cleavage and miRNA precursor processing [8,19,20]. It is also very important to explore the conservation and diversity of these molecular mechanism of XRN5s in other species.

5. Conclusions

In this study, we performed a large-scale identification and characterization of XRN proteins in the genomes of 5 plant species using Arabidopsis XRNs as references. A polygenetic tree with 23 XRNs was constructed, which revealed a novel member named XRN5. The conserved protein motif analysis revealed that a large region with motifs 11, 30, 22, 26, and 19 was mostly deleted in XRN4 and XRN5, and this region was partially lost in XRN2, SIXRN3-2, and PpXRN3-1. The detailed investigation in bipartite NLS suggested that all the XRN3 except SIXRN3-2 contained the potential bipartite NLS, while all the XRN4 lost the second key RR/KR motif. These results provide critical information associated with their sub-cellular localization, which is worthy of further exploration in the future. Finally, the transcriptomic data analysis revealed a global view of the XRNs' response to multiple environmental cues: some XRN homologs showed common expression patterns in response to the same abiotic stress, while most of them displayed a diverse response. Taken together, given the redundancy and functional diversity of XRNs in different species, XRN genes could be used as gene editing targets for precise stress-tolerant breeding.

Supplementary Materials: The following are available online at <https://www.mdpi.com/article/10.3390/d13120612/s1>. Figure S1. The pairwise structure alignment of two plant XRN proteins. The pairwise structure alignment of AtXRN3 (Orange) and OsXRN3 (Blue), displaying high similarity in the domains of alpha-helices and beta-sheets. The root mean square deviation (RMSD), TM-score, Score for structural similarity, sequence identity percentage (SI%), sequence similarity percentage (SS%), and the length of residue pairs structurally equivalent in the alignment were showed. Figure S2. Visualization of the selected conserved motif sequences. (A) Motif 15, which is shared among all 23 XRNs. (B) Motifs 30, 22, 26, and 19 that were frequently lost in XRN4, XRN5 and some of XRN3. (C) Motifs 27 and 29 were specifically detected in XRN4 proteins. (D) Motif 24 was specifically detected in XRN5 proteins. Figure S3. The conceived protein sequences of XRN 5'-3' exonuclease N-terminus. (A) The protein alignment of XRN 5'-3' exonuclease N-terminus that possess 5'-3' exonuclease activity, showing 10 most diverse species. The number ID of identified motifs corresponding to the conserved sequences were marked. (B) The motifs 14, 7, 4, 9, 21, 6, 18, and 1 in XRN 5'-3' exonuclease N-terminus domain. Figure S4. Cluster analysis of the *OsXRNs* expression pattern response to nutrition. Heat maps demonstrate the expression profiles of *OsXRNs* in response to Cd and P in rice shoot (A) and root (B).

Author Contributions: X.Y. and Y.B. designed the manuscript. W.S., Y.L., Y.N. and Y.W. analyzed the data and drew the figures. W.S., Y.B. and X.Y. wrote the manuscript. All authors have read and agreed to the published version of the manuscript.

Funding: This research was funded by Shanghai Pujiang Program, grant number 21PJ1407600; and supported by China Agriculture Research System of MOF and MARA.

Institutional Review Board Statement: Not applicable.

Informed Consent Statement: Not applicable.

Data Availability Statement: The data presented in this study are available in the article and supplementary materials.

Acknowledgments: We thank all the members of Yan Bao's lab and Xiang Yu's lab for their helpful discussions and comments on the manuscript. This work is supported by grant from Shanghai Pujiang Program (21PJ1407600 to X.Y.). The funders have no role in the study design, data collection and analysis, or the decision to publish the manuscript.

Conflicts of Interest: The authors declare no conflict of interest.

Abbreviations

NLS: Nuclear localization signal; PTGS: Post-transcriptional gene silencing; MEGA: Molecular Evolutionary Genetics Analysis; MW: Molecular weight; pI: isoelectric point; ABA: Abscisic acid; GA: gibberellin.

References

1. Nagarajan, V.K.; Jones, C.I.; Newbury, S.F.; Green, P.J. XRN 5'→3' Exoribonucleases: Structure, Mechanisms and Functions. *Biochim. Biophys. Acta (BBA)-Gene Regul. Mech.* **2013**, *1829*, 590–603. [[CrossRef](#)]
2. Chang, J.H.; Xiang, S.; Tong, L. Structures of 5'→3' Exoribonucleases. In *The Enzymes*; Elsevier: Amsterdam, The Netherlands, 2012; Volume 31, pp. 115–129. ISBN 978-0-12-404740-2.
3. Langeberg, C.J.; Welch, W.R.W.; McGuire, J.V.; Ashby, A.; Jackson, A.D.; Chapman, E.G. Biochemical Characterization of Yeast Xrn1. *Biochemistry* **2020**, *59*, 1493–1507. [[CrossRef](#)] [[PubMed](#)]
4. Xiang, S.; Cooper-Morgan, A.; Jiao, X.; Kiledjian, M.; Manley, J.L.; Tong, L. Structure and Function of the 5'→3' Exoribonuclease Rat1 and Its Activating Partner Rai1. *Nature* **2009**, *458*, 784–788. [[CrossRef](#)]
5. Pelechano, V.; Wei, W.; Steinmetz, L.M. Widespread Co-Translational RNA Decay Reveals Ribosome Dynamics. *Cell* **2015**, *161*, 1400–1412. [[CrossRef](#)] [[PubMed](#)]
6. Kastenmayer, J.P.; Green, P.J. Novel Features of the XRN-Family in Arabidopsis: Evidence That AtXRN4, One of Several Orthologs of Nuclear Xrn2p/Rat1p, Functions in the Cytoplasm. *Proc. Natl. Acad. Sci. USA* **2000**, *97*, 13985–13990. [[CrossRef](#)] [[PubMed](#)]
7. Hicks, G.R.; Raikhel, N.V. Protein import into the nucleus: An integrated view. *Annu. Rev. Cell Dev. Biol.* **1995**, *11*, 155–188. [[CrossRef](#)] [[PubMed](#)]
8. Zakrzewska-Placzek, M.; Souret, F.F.; Sobczyk, G.J.; Green, P.J.; Kufel, J. Arabidopsis Thaliana XRN2 Is Required for Primary Cleavage in the Pre-Ribosomal RNA. *Nucleic Acids Res.* **2010**, *38*, 4487–4502. [[CrossRef](#)]
9. Merret, R.; Nagarajan, V.K.; Carpentier, M.-C.; Park, S.; Favory, J.-J.; Descombin, J.; Picart, C.; Charng, Y.; Green, P.J.; Deragon, J.-M.; et al. Heat-Induced Ribosome Pausing Triggers mRNA Co-Translational Decay in Arabidopsis Thaliana. *Nucleic Acids Res.* **2015**, *43*, 4121–4132. [[CrossRef](#)]
10. Yu, X.; Willmann, M.R.; Anderson, S.J.; Gregory, B.D. Genome-Wide Mapping of Uncapped and Cleaved Transcripts Reveals a Role for the Nuclear mRNA Cap-Binding Complex in Cotranslational RNA Decay in Arabidopsis. *Plant Cell* **2016**, *28*, 2385–2397. [[CrossRef](#)]
11. Carpentier, M.-C.; Deragon, J.-M.; Jean, V.; Be, S.H.V.; Bousquet-Antonelli, C.; Merret, R. Monitoring of XRN4 Targets Reveals the Importance of Cotranslational Decay during Arabidopsis Development. *Plant Physiol.* **2020**, *184*, 1251–1262. [[CrossRef](#)]
12. Krzysztan, M.; Zakrzewska-Placzek, M.; Kwasnik, A.; Dojer, N.; Karlowski, W.; Kufel, J. Defective XRN 3-mediated Transcription Termination in Arabidopsis Affects the Expression of Protein-coding Genes. *Plant J.* **2018**, *93*, 1017–1031. [[CrossRef](#)]
13. Kurihara, Y. Activity and Roles of Arabidopsis Thaliana XRN Family Exoribonucleases in Noncoding RNA Pathways. *J. Plant Res.* **2017**, *130*, 25–31. [[CrossRef](#)]
14. Zhang, X.; Zhu, Y.; Liu, X.; Hong, X.; Xu, Y.; Zhu, P.; Shen, Y.; Wu, H.; Ji, Y.; Wen, X.; et al. Suppression of Endogenous Gene Silencing by Bidirectional Cytoplasmic RNA Decay in Arabidopsis. *Science* **2015**, *348*, 120–123. [[CrossRef](#)]
15. Souret, F.F.; Kastenmayer, J.P.; Green, P.J. AtXRN4 Degrades mRNA in Arabidopsis and Its Substrates Include Selected miRNA Targets. *Mol. Cell* **2004**, *15*, 173–183. [[CrossRef](#)] [[PubMed](#)]
16. Gazzani, S. A Link between mRNA Turnover and RNA Interference in Arabidopsis. *Science* **2004**, *306*, 1046–1048. [[CrossRef](#)]
17. Gregory, B.D.; O'Malley, R.C.; Lister, R.; Urich, M.A.; Tonti-Filippini, J.; Chen, H.; Millar, A.H.; Ecker, J.R. A Link between RNA Metabolism and Silencing Affecting Arabidopsis Development. *Dev. Cell* **2008**, *14*, 854–866. [[CrossRef](#)]
18. Liu, Y.; Gao, W.; Wu, S.; Lu, L.; Chen, Y.; Guo, J.; Men, S.; Zhang, X. AtXRN4 Affects the Turnover of Chosen miRNA*s in Arabidopsis. *Plants* **2020**, *9*, 362. [[CrossRef](#)] [[PubMed](#)]
19. Kurihara, Y.; Schmitz, R.J.; Nery, J.R.; Schultz, M.D.; Okubo-Kurihara, E.; Morosawa, T.; Tanaka, M.; Toyoda, T.; Seki, M.; Ecker, J.R. Surveillance of 3' Noncoding Transcripts Requires FIERY1 and XRN3 in Arabidopsis. *G3 Genes Genomes Genet.* **2012**, *2*, 487–498. [[CrossRef](#)]
20. Gy, I.; Gascioli, V.; Laressergues, D.; Morel, J.-B.; Gombert, J.; Proux, F.; Proux, C.; Vaucheret, H.; Mallory, A.C. Arabidopsis FIERY1, XRN2, and XRN3 Are Endogenous RNA Silencing Suppressors. *Plant Cell* **2007**, *19*, 3451–3461. [[CrossRef](#)] [[PubMed](#)]
21. Kwasnik, A.; Wang, V.Y.-F.; Krzysztan, M.; Gozdek, A.; Zakrzewska-Placzek, M.; Stepniak, K.; Poznanski, J.; Tong, L.; Kufel, J. Arabidopsis DXO1 Links RNA Turnover and Chloroplast Function Independently of Its Enzymatic Activity. *Nucleic Acids Res.* **2019**, *47*, 4751–4764. [[CrossRef](#)]
22. Yu, X.; Willmann, M.R.; Vandivier, L.E.; Trefely, S.; Kramer, M.C.; Shapiro, J.; Guo, R.; Lyons, E.; Snyder, N.W.; Gregory, B.D. Messenger RNA 5' NAD⁺ Capping Is a Dynamic Regulatory Epitranscriptome Mark That Is Required for Proper Response to Abscisic Acid in Arabidopsis. *Dev. Cell* **2021**, *56*, 125–140. [[CrossRef](#)] [[PubMed](#)]
23. Sharma, S.; Yang, J.; Grudzien-Nogalska, E.; Kiledjian, M. Xrn1 Is a DeNADding Enzyme Modulating Mitochondrial NAD Levels. *Mol. Biol.* **2021**. [[CrossRef](#)]
24. Roman, G.; Lubarsky, B.; Kieber, J.J.; Rothenberg, M.; Ecker, J.R. Genetic analysis of ethylene signal transduction in Arabidopsis thaliana: Five novel mutant loci integrated into a stress response pathway. *Genetics* **1995**, *139*, 1393–1409. [[CrossRef](#)]
25. Wawer, I.; Golisz, A.; Sulkowska, A.; Kawa, D.; Kulik, A.; Kufel, J. mRNA Decapping and 5'-3' Decay Contribute to the Regulation of ABA Signaling in Arabidopsis Thaliana. *Front. Plant Sci.* **2018**, *9*, 312. [[CrossRef](#)]
26. Merret, R.; Descombin, J.; Juan, Y.; Favory, J.-J.; Carpentier, M.-C.; Chaparro, C.; Charng, Y.; Deragon, J.-M.; Bousquet-Antonelli, C. XRN4 and LARP1 Are Required for a Heat-Triggered mRNA Decay Pathway Involved in Plant Acclimation and Survival during Thermal Stress. *Cell Rep.* **2013**, *5*, 1279–1293. [[CrossRef](#)]

27. Nagarajan, V.K.; Kukulich, P.M.; von Hagel, B.; Green, P.J. RNA Degradomes Reveal Substrates and Importance for Dark and Nitrogen Stress Responses of Arabidopsis XRN4. *Nucleic Acids Res.* **2019**, *47*, 9216–9230. [[CrossRef](#)]
28. Stecher, G.; Tamura, K.; Kumar, S. Molecular Evolutionary Genetics Analysis (MEGA) for MacOS. *Mol. Biol. Evol.* **2020**, *37*, 1237–1239. [[CrossRef](#)] [[PubMed](#)]
29. Chen, C.; Chen, H.; Zhang, Y.; Thomas, H.R.; Frank, M.H.; He, Y.; Xia, R. TBtools: An Integrative Toolkit Developed for Interactive Analyses of Big Biological Data. *Mol. Plant* **2020**, *13*, 1194–1202. [[CrossRef](#)]
30. Lescot, M. PlantCARE, a Database of Plant Cis-Acting Regulatory Elements and a Portal to Tools for in Silico Analysis of Promoter Sequences. *Nucleic Acids Res.* **2002**, *30*, 325–327. [[CrossRef](#)]
31. Perroud, P.; Haas, F.B.; Hiss, M.; Ullrich, K.K.; Alboresi, A.; Amirebrahimi, M.; Barry, K.; Bassi, R.; Bonhomme, S.; Chen, H.; et al. The *Physcomitrella Patens* Gene Atlas Project: Large-scale RNA-seq Based Expression Data. *Plant J.* **2018**, *95*, 168–182. [[CrossRef](#)]
32. Zouine, M.; Maza, E.; Djari, A.; Lauvernier, M.; Frasse, P.; Smouni, A.; Pirrello, J.; Bouzayen, M. TomExpress, a Unified Tomato RNA-Seq Platform for Visualization of Expression Data, Clustering and Correlation Networks. *Plant J.* **2017**, *92*, 727–735. [[CrossRef](#)]
33. Machado, F.B.; Moharana, K.C.; Almeida-Silva, F.; Gazara, R.K.; Pedrosa-Silva, F.; Coelho, F.S.; Grativol, C.; Venancio, T.M. Systematic Analysis of 1298 RNA-Seq Samples and Construction of a Comprehensive Soybean (*Glycine Max*) Expression Atlas. *Plant J.* **2020**, *103*, 1894–1909. [[CrossRef](#)] [[PubMed](#)]
34. Kawahara, Y.; Oono, Y.; Wakimoto, H.; Ogata, J.; Kanamori, H.; Sasaki, H.; Mori, S.; Matsumoto, T.; Itoh, T. TENOR: Database for Comprehensive mRNA-Seq Experiments in Rice. *Plant Cell Physiol.* **2016**, *57*, e7. [[CrossRef](#)] [[PubMed](#)]
35. Hoopes, G.M.; Hamilton, J.P.; Wood, J.C.; Esteban, E.; Pasha, A.; Vaillancourt, B.; Provart, N.J.; Buell, C.R. An Updated Gene Atlas for Maize Reveals Organ-specific and Stress-induced Genes. *Plant J.* **2019**, *97*, 1154–1167. [[CrossRef](#)]
36. Jumper, J.; Evans, R.; Pritzel, A.; Green, T.; Figurnov, M.; Ronneberger, O.; Tunyasuvunakool, K.; Bates, R.; Žídek, A.; Potapenko, A.; et al. Highly Accurate Protein Structure Prediction with AlphaFold. *Nature* **2021**, *596*, 583–589. [[CrossRef](#)] [[PubMed](#)]